ELSEVIER

Neurocomputing 13 (1996) 135–149

NEUROCOMPUTING

Generalized Hopfield networks for associative memories with multi-valued stable states

Jacek M. Zurada [a,*], Ian Cloete [b], Etienne van der Poel [b]

[a] *Department of Electrical Engineering, University of Louisville, Louisville, KY 40292, USA*
[b] *Department of Computer Science, University of Stellenbosch, Stellenbosch 7600, South Africa*

Received 24 February 1995; accepted 11 September 1995

Abstract

Hopfield networks with fully connected standard neurons can be generalized by replacing bi-level activation functions with their multilevel counterparts. Multilevel neuron characteristics are discussed in the paper with emphasis on their inflection points. It is shown that an activation function possessing $(N+1)$-levels yields $N+1$ minima and N saddle points of the computational energy function when two generalized neurons are used in a conventional bi-stable connection. Analytical results for parameter constraints and energy function properties are discussed for binary and ternary characteristics of neurons. Gradient fields indicating basins of attraction for continuous-time networks are used to illustrate dynamical relationships during network convergence to stable points. Results indicate that generalized Hopfield networks can be used for multilevel signal processing and smoothing of planar images.

Keywords: Hopfield network; Associative memory; Multivalued neural networks; Multistable flip flops

1. Introduction

Most neural networks are defined as consisting of 'two-state' neurons and evaluated accordingly. Neurons' activation functions in such networks are considered as having sigmoidal (soft-limiting) or signum-type (hard-limiting) shape. Much more diversified and still stable network behavior, however, can be observed when multilevel neuron characteristics are used. While these networks, called here generalized Hopfield networks (GHN), preserve the global stability properties of original Hopfield networks, they display a multiplicity of stable states. This paper outlines a formal framework of the

* Corresponding author. Email: jmzura02@starbaselouisville.edu

SSDI 0925-2312(96)00086-0

GHN concept and discusses basic features of such networks. Both formal propositions and illustrative discussions using the energy concept demonstrate substantial potential for GHNs as multilevel image processors. In addition, such networks can be directly applicable in multi-valued logic circuits.

2. Activation functions of a GHN neuron

Inspection of a continuous-time neuron activation function shown in Fig. 1(a) indicates that the function possesses a single inflection point. The activation function is of the standard form as in (1)

$$f(x) = 2f_s(x) - 1 \tag{1}$$

where $f_s(x) = (1 + e^{-\lambda x})^{-1}$.

Consider a set of 3 desired inflection points for the activation function of a multilevel neuron. This yields the activation function for $N = 2$ of the following form

$$f(x, 2) \triangleq f_s\left(x - \frac{1}{2}\right) + f_s\left(x + \frac{1}{2}\right) - 1 \tag{2}$$

with three potential inflection points equal to $-\frac{1}{2}$, 0, and $\frac{1}{2}$. Notably, all inflection points only occur for λ values large enough. It is shown below that for $N = 2$ it is required that $\lambda > 2\ln(2 + \sqrt{3})$.

For the discussion to follow refer to Fig. 2 showing $f(x, 2)$ and its derivatives f', f'', and f''' at $\lambda = \lambda_{crit}$ and $\lambda = 3 > \lambda_{crit}$. When λ is not large enough, equation $f''(x, 2) = 0$ has only one root at the origin. Since $f''(x, 2) = 0$ changes sign at inflection points, we require the existence of three solutions of $f''(x, 2) = 0$. In order to satisfy this condition, four solutions of equation $f'''(x, 2) = 0$ must exist, requiring also $f'''(0, 2) > 0$. Using (2) we obtain

$$f'''(0, 2) = f_s'''\left(\frac{1}{2}\right) + f_s'''\left(-\frac{1}{2}\right) \tag{3}$$

Since $f_s'''(\frac{1}{2}) = f_s'''(-\frac{1}{2})$ we have

$$f'''(0, 2) = 2f_s'''\left(\frac{1}{2}\right) \tag{4}$$

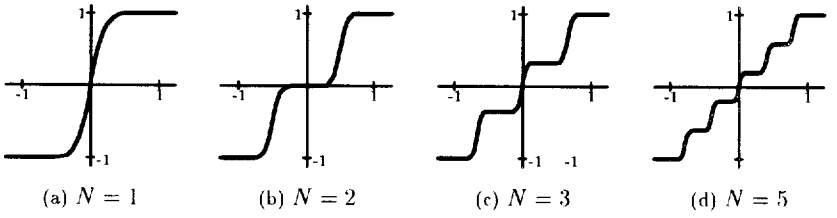

Fig. 1. GHN activation functions for: (a) $N = 1$ (b) $N = 2$ (c) $N = 3$, and (d) $N = 5$.

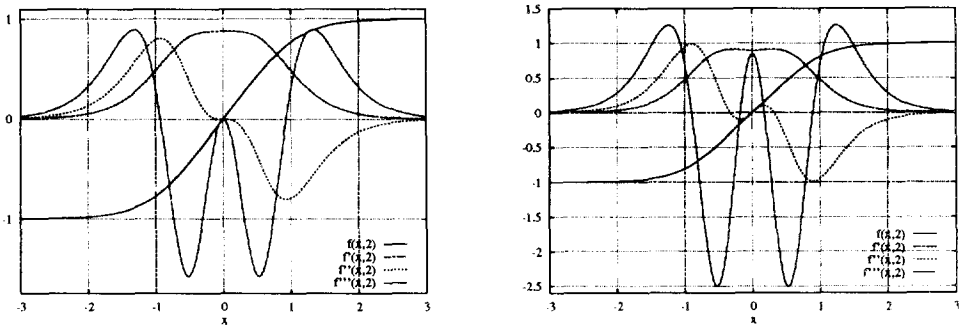

(a) (b)

Fig. 2. GHN activation functions for $N = 2$ and their derivatives (a) $\lambda = \lambda_{crit}$, (b) $\lambda = 3 > \lambda_{crit}$ as in (10).

Further, it can be shown that

$$f_s'''(x) = \lambda^3 f_s(x)(1 - f_s(x))\left[6f_s^2(x) - 6f_s(x) + 1\right] \tag{5}$$

The critical value for λ is therefore when the term in square brackets in (5) becomes greater than zero for $y \triangleq f_s(x)|_{x=\frac{1}{2}}$ since all other terms in (5) are greater than zero yielding

$$f_s\left(\frac{1}{2}\right) = y = \frac{3 \pm \sqrt{3}}{6} \tag{6}$$

Taking the smaller root $(3 - \sqrt{3})/6$ yields a negative value $\lambda < -2\ln(2 + \sqrt{3})$, which is invalid, because it is assumed that λ is positive. Plugging the larger of the two roots of (6) equal to $(3 + \sqrt{3})/6$ into the inverse of the activation function $f_s(x)$

$$x = f_s^{-1}(y) = -\frac{1}{2}\ln\frac{1-y}{y} \tag{7}$$

we obtain the condition

$$\frac{1}{2} > -\frac{1}{\lambda}\ln(2 - \sqrt{3}) \tag{8}$$

This condition is satisfied for λ exceeding the critical value of

$$\lambda_{crit} = 2\ln(2 + \sqrt{3}) \approx 2.6339 \tag{9}$$

Noticing that this is the minimum λ value producing two additional inflection points symmetrical to the origin, it can be stated that GHNs for $N = 2$ have gainful properties for λ of much higher values than λ_{crit}.

Fig. 3(a) shows activation functions $f(x, 2)$ for the subcritical case $\lambda = 1$ for which desired inflection points are not yet formed, and the critical case of $\lambda = \lambda_{crit}$. It also includes two activation functions with three inflection points for λ values above λ_{crit}. Figs. 3(b) and (c) illustrate examples of functions $f'(x, 2)$ and $f''(x, 2)$, respectively, produced for the same λ values as used in Fig. 3(a).

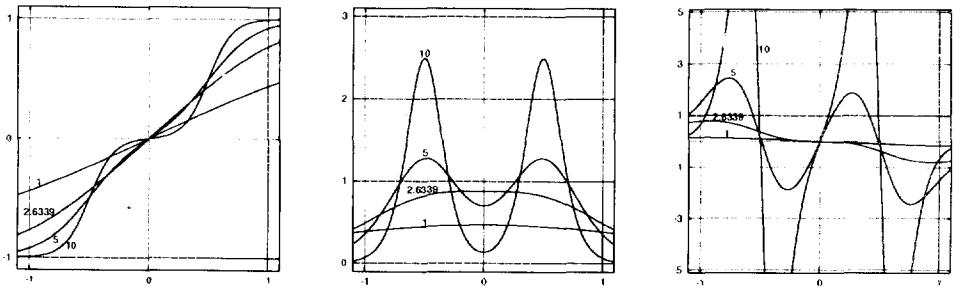

Fig. 3. Activation functions and their derivatives for $N = 2$ (a) $f(x, 2)$ (b) $f'(x, 2)$ (c) $f''(x, 2)$ (λ values are indicated in the figure).

Combining shifted high-gain functions $f_s(x)$ and scaling them properly results in Table 1 which lists desired inflection points and formulas for the activation functions $f(x, N)$ for $N = 1, \ldots, 5$. Note that the inflection points listed are those involved in horizontal shifting of each $f_s(x)$.

To summarize, the general formulae for the inflection points, θ_i, and corresponding activation functions for an arbitrary value of N is

$$\theta_i = \frac{1}{N} + 2\frac{i-1}{N} - 1, \quad \text{for } i = 1, 2, \ldots, N \tag{10}$$

$$f(x, N) = \frac{2}{N}\sum_{i=1}^{N} f_s(x + \theta_i) - 1 \tag{11}$$

Figs. 1(b), (c), and (d) illustrate examples of the activation functions $f(x, N)$ of multilevel neurons for $N = 2$, 3 and 5. It is assumed and valid for further considerations that the steepness coefficient, λ, is large enough for the inflection points of the functions $f(x, N)$ as in (11) to exist at these locations as specified by (10). The actual value of the x-coordinates of the inflection points beyond the origin slightly differ from those stated in the table when λ takes finite values. When $\lambda \to \infty$, however, these location assymptotically approach the ones listed in the table or specified by (11).

Table 1
Desired inflection points and activation functions of GHN neurons

N	Selected inflection points	$f(x, N)$
1	0	$2(\frac{1}{1})f_s(x) - 1$
2	$-\frac{1}{2}, \frac{1}{2}$	$2(\frac{1}{2})(f_s(x-\frac{1}{2}) + f_s(x+\frac{1}{2})) - 1$
3	$-\frac{2}{3}, 0, \frac{2}{3}$	$2(\frac{1}{3})(f_s(x-\frac{2}{3}) + f_s(x) + f_s(x+\frac{2}{3})) - 1$
4	$-\frac{3}{4}, -\frac{1}{4}, \frac{1}{4}, \frac{3}{4}$	$2(\frac{1}{4})(f_s(x-\frac{3}{4}) + f_s(x-\frac{1}{4}) + f_s(x+\frac{1}{4}) + f_s(x+\frac{3}{4})) - 1$
5	$-\frac{4}{5}, -\frac{2}{5}, 0, \frac{2}{5}, \frac{4}{5}$	$2(\frac{1}{5})(f_s(x-\frac{4}{5}) + f_s(x-\frac{2}{5}) + f_s(x) + f_s(x+\frac{2}{5}) + f_s(x+\frac{4}{5})) - 1$

3. Generalized Hopfield networks

It is further assumed that GHNs are networks with weight matrices which fulfill the original assumptions of Hopfield networks, ie. their weight matrices are symmetrical and contain zeroes on the diagonal [1,2]. Such neural networks have no self-feedback, so they are 'almost' fully connected feedback networks. Their recurrent operation during the recall phase can be analyzed either in discrete-time or continuous-time mode [3].

It should be noted that under these assumptions for the activation functions of multilevel neurons, the GHNs still obey the energy minimization property. This is due to the fact that the monotonicity of $f(x, N)$ is preserved for any N value. GHNs are therefore absolutely stable as are the original Hopfield networks. Obviously, the condition of stability requires nullification of the diagonal of the weight matrix as well as its symmetry. However, much richer dynamic behaviour is expected for the GHNs due to the expansion of the state space beyond binary values which apply for a standard activation function case [4–6]. In this perspective, Hopfield networks can be considered as a sub-class of GHNs, in the entailing $N = 1$ case only.

4. Equilibrium points of GHN with two neurons

This section focuses on the discussion of equilibrium points which occur in GHNs. There are 2^n vertices of the hypercube in the state space of a discrete-time Hopfield network employing n two-state binary neurons ($N = 1$). The same architecture with ternary hard-limiting neurons described with $f(x, 2)$ in (11) for $\lambda \to \infty$, would possess 3^n stable states. Our focus is on continuous-time behavior of GHNs. In order to succinctly capture the underlying principles of GHN, the discussion below is limited to a bi-stable flip-flop architecture with the bi-stable neurons replaced by multilevel computing elements such that $N > 1$.

Consider a bi-stable flip-flop as shown in Fig. 4. Its weight matrix is [7]

$$\mathbf{W} = \begin{bmatrix} 0 & 1 \\ 1 & 0 \end{bmatrix} \tag{12}$$

The dynamics of the network can be explained by inspection of Fig. 5 showing both the activation function $f(x, N)$ for $N = 1$, and the line $v = x$. Although the network of

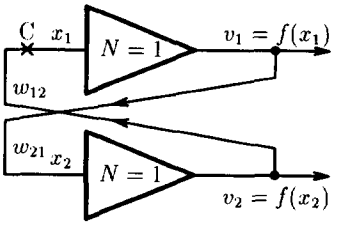

Fig. 4. Conventional two-neuron Hopfield network behaving as a bi-stable flip-flop.

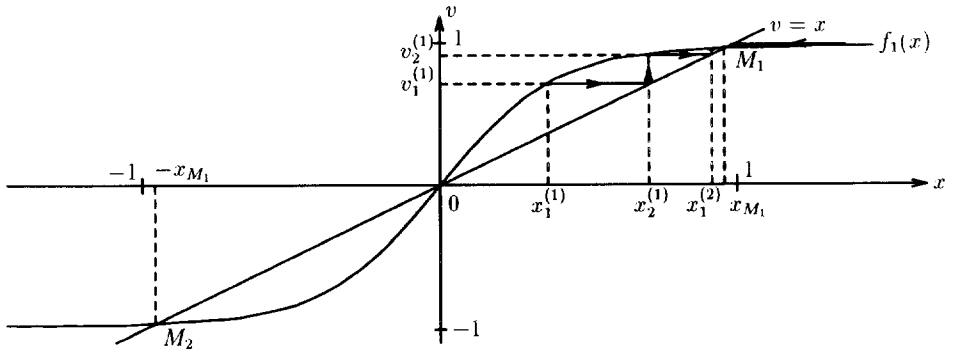

Fig. 5. Discussion of equilibrium points for bi-stable flip-flop (case $N = 1$).

Fig. 5 is static, its time-domain behavior can be illustrated by considering the following recurrences (superscripts refer to time step numbers): The initial input value to the neuron 1, $x_1^{(1)} < x_{M1}$, produces output $v_1^{(1)}$. Since $w_{21} = 1$, $v_1^{(1)}$ now becomes $x_2^{(1)}$ and it produces a response of the second neuron equal to $v_2^{(1)}$. This transfers, through weight $w_{12} = 1$ to the input of the first neuron as $x_1^{(2)}$ and the recursive update restarts. It can be seen that this recursive computing continues until it ends at a point $M1(x_{M1}, v_{M1})$. It is similarly easy to verify that recursions originating at $x_1^{(1)} > x_{M1}$ also terminate at $M1$. It can thus be concluded that $M1$ is a stable equilibrium point of this configuration.

Although this discussion does not capture the detailed network dynamics vs. time since dynamical components (capacitors) are removed from consideration, it provides insight into the type of convergence exhibited by the actual network. To bridge the recursive update scheme discussed above with the performance of an actual network it might be helpful to cut the connection of the network in Fig. 4 at point C and to analyze the impact of an open feedback loop connection. It can now be seen that the input $x_1^{(1)}$ is mapped into the output $v_2^{(1)}$ in an open-loop configuration. Since the loop is actually closed and C represents only a fictitious cut, $v_2^{(1)}$ enforces identical input to the neuron 1, i.e. $v_2^{(1)} = x_1^{(2)}$ due to the existing connection. The recursion then restarts and it continues until point $M1$ is reached. A similar discussion leads to the conclusion that $M2$ in the third quadrant is another stable point of this network.

Relating these properties to the stability theorems of nonlinear systems has been shown in [1] and [2] that both $M1$ and $M2$ are minima of the Lyapunov function called the computational energy function, $E(v_1, v_2)$. It can also be noticed that the origin, O, is an unstable equilibrium point which cannot be reached through recursions from any starting point. This point corresponds to the saddle point of the energy function. Although the gradient vector of the energy function $E(v_1, v_2)$ vanishes at point O, the weight matrix is indefinite there, thus yielding a saddle point of an energy landscape at the origin [8]. In summary, there exists one saddle point and two minima for an energy function describing the network from Fig. 4 with conventional bi-stable neurons.

Let us discuss the type of equilibrium points occurring for $N > 1$. Fig. 6 depicts an example of the activation function of a GHN neuron for $N = 4$ and the line $v = x$ for the

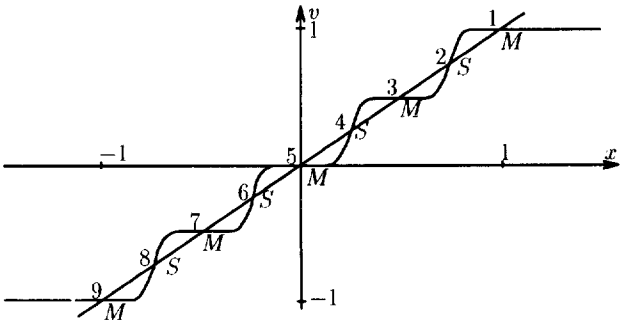

Fig. 6. Illustration to discussion of equilibrium points for $N > 1$ (Case $N = 4$).

network configuration as shown in Fig. 4, but now using neurons with 5 levels. The network possesses the following properties: Moving from the top right of the figure a triplet of points {1, 2, 3} can be identified as identical in character to the one shown in Fig. 5. Points 1 and 3 are thus stable minima, and 2 is an unstable saddle point. Triplets {3, 4, 5}, {5, 6, 7}, and {7, 8, 9} can be characterized similarly with each first and third member of the set being two stable points which are minima, and the middle member being an unstable saddle. It can therefore be concluded that the closed-loop network has 5 distinct stable minima and 4 unstable saddle points.

In general, it can be stated that if a network configured as shown in Fig. 4 consists of neurons whose activation functions have N inflection points at which the slope of the function $f(x, N)$ is high enough, then the network energy function has N saddle points and $N + 1$ minima. Further, note that the minimum is always to the rightmost position and minima intertwine (or alternate) with saddles. Inflection points of the activation function, such as even-numbered points of Fig. 6, correspond to the saddle locations of the network's energy function.

5. Critical parameter values

In further discussion we utilize the energy function to gain better insight into the dynamic behaviour of the network. The energy function for the two-neuron GHN flip-flop is defined as [7]

$$E(\mathbf{v}) = -\frac{1}{2}\mathbf{v}^t \mathbf{W}\mathbf{v} + \sum_{i=1}^{2} G_i \int_0^{v_i} f^{-1}(z, N)\, \mathrm{d}z \tag{13}$$

Using the weight matrix containing two identical weights $w_{12} = w_{21} = w$, the gradient vector of the energy function is equal to

$$\nabla E(\mathbf{v}) = \begin{bmatrix} -wv_2 + G_1 f^{-1}(v_1, N) \\ -wv_1 + G_2 f^{-1}(v_2, N) \end{bmatrix} \tag{14}$$

In order to evaluate minima and saddles of the energy function, conditions at stationary points being solutions of the equation $\nabla E(\mathbf{v}) = 0$ need to be analyzed using

Table 2
Critical values of λ for various N

N	2	3	4	5	6	7
λ_{crit}	2.6339	4.3634	5.8329	7.2921	8.7506	10.2090

the Hessian matrix determinant for this case. Since $d[f^{-1}(u)]/du = 1/f'(u)$, the Hessian of $E(\mathbf{v})$ is

$$H_{E(\mathbf{v})} = \begin{bmatrix} \dfrac{G_1}{\dfrac{\partial f(v_1, N)}{\partial v_1}} & -w \\ -w & \dfrac{G_2}{\dfrac{\partial f(v_2, N)}{\partial v_2}} \end{bmatrix} \tag{15}$$

In order for the GHNs to possess the desired number of minima certain critical parameter values should exist. As indicated in Section 2, function $f(x, N)$ should have $2N-1$ inflection points at which $f''(x, N) = 0$. We have introduced λ_{crit} as the smallest value of the steepness factor, λ, for which all required inflection points exist. Table 2 lists critical values of λ for $N = 2, 3, \ldots, 7$. For $N > 2$ the values have been calculated numerically.

Another set of conditions ensuring appropriate functioning of the GHN from Fig. 4 is related to the existence of the appropriate number of minima and saddles of the energy functions. These conditions relate λ values with other network coefficients involved in expression (13), namely G and w values. They are evaluated below for various N when the Hessian expression can still be handled analytically.

The conditions for existence of stationary points depend on the determinant of the Hessian of E. For a saddle point of E to exist the determinant must be less than zero. For a minimum of E the determinant must be greater than zero and the second partial derivative with respect to v greater than zero. For $N = 1$ the gradient (14) equals

$$\nabla E(\mathbf{v}) = \begin{bmatrix} -wv_2 + G_1 \dfrac{1}{\lambda} \ln \dfrac{1+v_1}{1-v_1} \\ -wv_1 + G_2 \dfrac{1}{\lambda} \ln \dfrac{1+v_2}{1-v_2} \end{bmatrix} \tag{16}$$

where $f^{-1}(\mathrm{v}) = (1/\lambda) \ln(1+v)/(1-v)$ is the inverse of the activation function $f(x, 1) = 2f_s(x) - 1$. The Hessian matrix of E now becomes

$$H_{E(\mathbf{v})} = \begin{bmatrix} \dfrac{2G_1}{\lambda(1-v_1)(1+v_1)} & -w \\ -w & \dfrac{2G_2}{\lambda(1-v_2)(1+v_2)} \end{bmatrix} \tag{17}$$

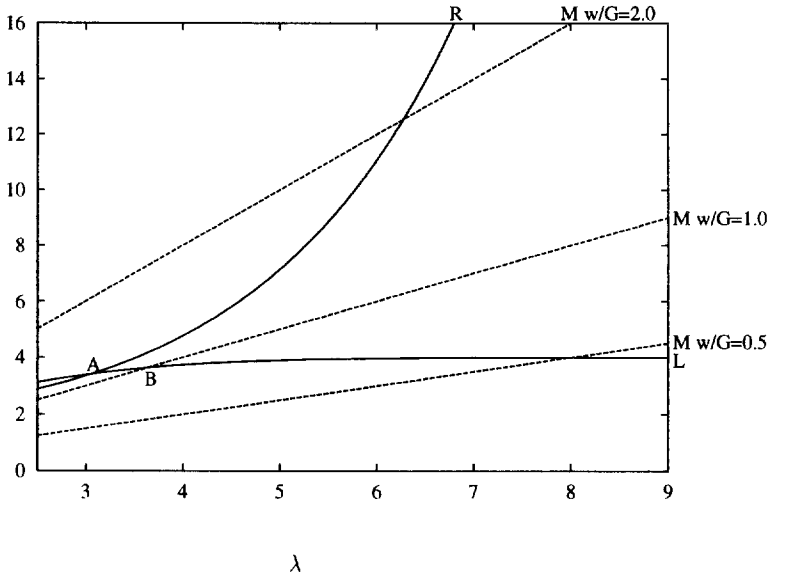

Fig. 7. Graphical interpretation of conditions for λ for which saddles of $E(\mathbf{v})$ exist (case $N = 2$).

By analyzing the existence condition of the saddle at the origin it can be shown that for $N = 1$ det $H < 0$ for $\lambda w/G > 2$. For $N = 2$, saddle points of $E(v_1, v_2)$ exist at $v_1 = v_2 = \pm 0.5$ as $\lambda \to \infty$, and a single minimum exists at the origin. For this case the following constraints must be met

$$\frac{4(1+e^{-\lambda})^2}{1+6e^{-\lambda}+e^{-2\lambda}} < \frac{\lambda w}{G} < \frac{(1+e^{\lambda/2})^2}{2e^{\lambda/2}} \tag{18}$$

The boundaries of (18) can be interpreted graphically as functions as shown in Fig. 7. The figure shows the upper (**R**) and lower (**L**) bounds for the value of $\lambda w/G$. From the figure the absolute minimum for the existence of saddles is 3.0571 (point **A**). For

Table 3
Values of λ_{Ecrit} and coordinates of saddles, in $E(\mathbf{v})$ for $N = 1, 2, \ldots, 7$

N	λ_{Ecrit}	v at saddle	N	λ_{Ecrit}	v at saddle
1	2.0000	0.000	6	6.4909	0.153
2	3.5764	0.428		7.7435	0.479
3	3.6754	0.000		10.6588	0.807
	5.3305	0.615	7	6.8821	0.000
4	5.2066	0.224		7.5108	0.271
	7.1059	0.711		9.0336	0.554
5	7.6570	0.000		12.4353	0.835
	6.4571	0.376			
	8.8823	0.769			

$w/G = 1$, the minimum value of λ is 3.5764 (point **B**). Realising that the boundaries (18) must be satisfied, applicable constraints can be found for λ given the w/G value. Comparing conditions on the existence of the inflection points with those discussed in Section 2 for case $N = 2$ it can be seen that $\lambda > \lambda_{crit} = 2.6339$ from Table 2 is a necessary condition. The existence of the saddles for $N = 2$ requires $\lambda > 3.5764$, which can be considered as a sufficient condition. Numerical analysis of sufficient conditions for λ and $N > 2$ has been carried out with regard to the lowest values of λ for the existence of all saddle points of the energy function at all inflection points. These values are called λ_{Ecrit}. The results are summarized in Table 3 which also list saddle point coordinates for $v > 0$ with $\lambda = \lambda_{Ecrit}$.

6. Evaluation of energy landscapes and basins of attraction

The energy function analysis throughout this paper has provided the insight into the stability and dynamics of the 2-neuron GHNs. This section focuses on visualization of

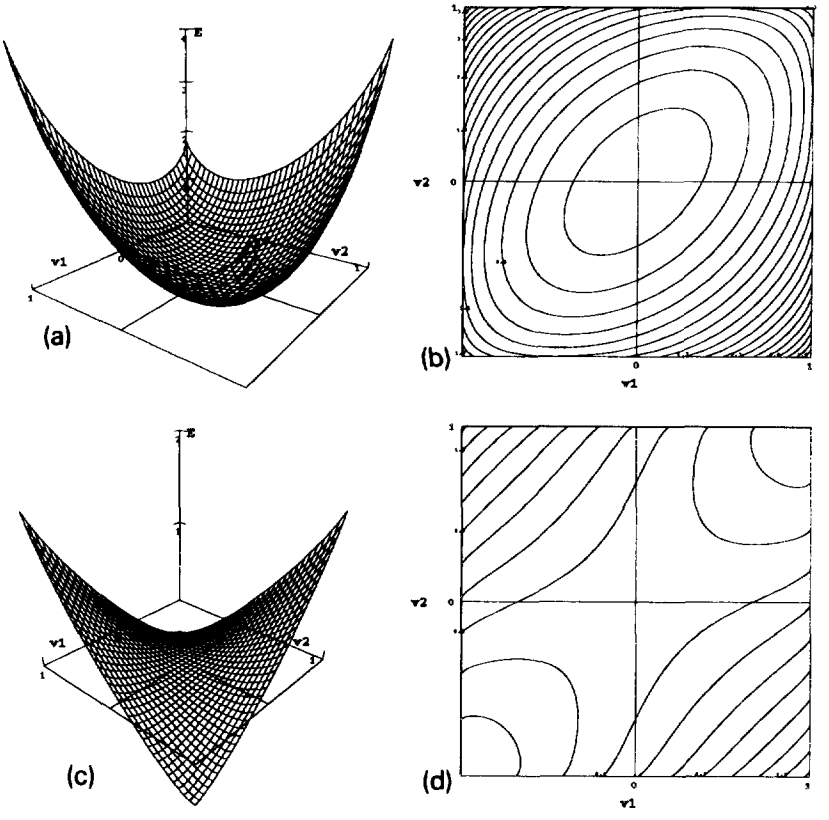

Fig. 8. Energy functions for different conditions (a) surface $N = 1$, $\lambda = 1$ (b) contour map $N = 1$, $\lambda = 1$ (c) surface $N = 1$, $\lambda = 5$ (d) contour map $N = 1$, $\lambda = 5$.

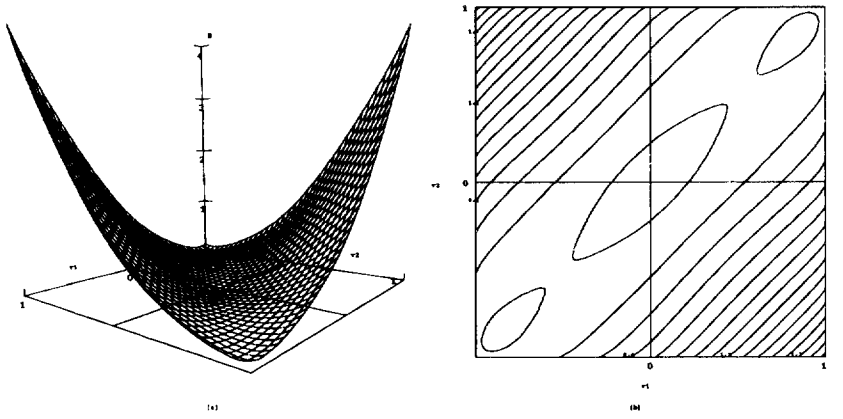

Fig. 9. Energy functions for $N = 2$, $\lambda = 5$ (a) surface (b) contour map.

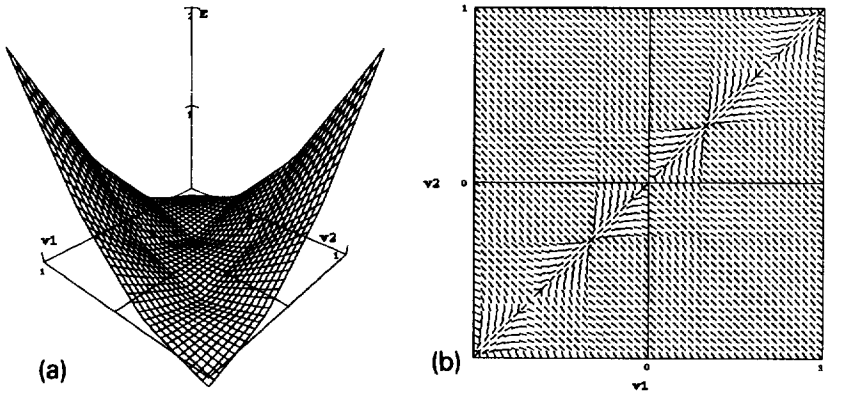

Fig. 10. (a) Energy surface for $N = 3$, $\lambda = 40$ (b) Vector field for $N = 3$, $\lambda = 20$.

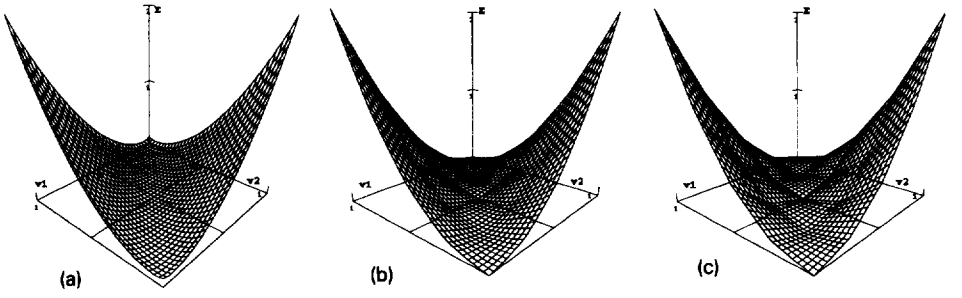

Fig. 11. Energy surfaces for $N = 4$ (a) $\lambda = 5$ (b) $\lambda = 20$ (c) $\lambda = 90$.

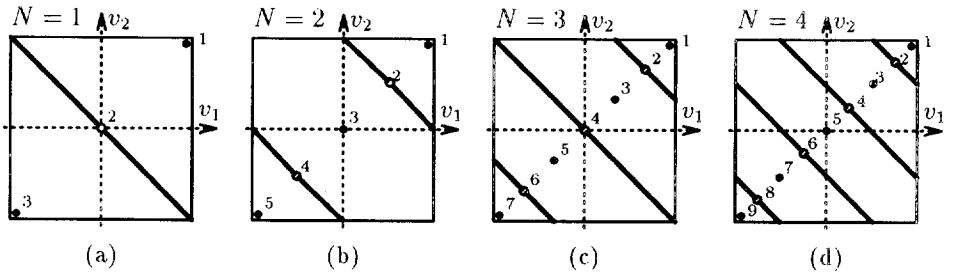

Fig. 12. Basins of attraction for various N values (a) $N = 1$ (b) $N = 2$ (c) $N = 3$ (d) $N = 4$.

the energy surfaces, on discussion of relevant gradient fields, and networks' basins of attraction for different computational conditions. To qualitatively illustrate the behaviour of GHNs and their stability properties for graphs in this section assume the condition $G = w = 1$.

Figs. 8(a) and (b) show the energy landscape and the respective contour map for a subcritical case $\lambda = 1$ when $N = 1$. Due to a low λ value no saddle point has developed which would separate two minima for this potentially bi-stable configuration. For $\lambda = 5 > \lambda_{Ecrit}$, the bi-stability property can easily be seen from Figs. 8(c) and (d).

Fig. 9 provides the energy function along with its contour map for $N = 2$, $\lambda = 5$. The energy function exhibits three distinct minima and two saddle points. Fig. 10(a) illustrates the energy function for $N = 3$, $\lambda = 40$. There are 3 saddle points and 4 minima for this high-gain case. Fig. 11 depicts the case of $N = 4$ for three distinct values of λ. Subcritical, too low value of λ ($\lambda = 5$ in this case) leads to the absence of desired stationary points as shown in Fig. 11(a). Such points have been able to develop for the network with $\lambda = 20$, as shown in Fig. 11(b). A much more 'crispy' energy landscape is produced in Fig. 11(c) for $\lambda = 90$. Although minima of $E(\mathbf{v})$ are still attractive in the two latter cases in a similar way, stationary points are now easier to distinguish.

Fig. 10(b) shows the vector fields of a high-gain GHN for $N = 3$. Arrows pointing in directions of system transients are indicative of the directions of the slope of the energy function [3,9]. Basins of attraction are also distinguishable from this figure for the discussed network.

In the case of a symmetrical weight matrix and $G_1 = G_2$, basins of attraction can be sketched as in Fig. 12. It can be seen that the basins are symmetrical with respect to the diagonal $v_1 = v_2$ and bordered by straight lines containing the saddle points and having a slope of -1. It can be seen that odd numbered attractors on the figure will be the endpoints of any trajectory originating in a given region.

7. Image restoration application

Multilevel neurons have recently been applied successfully for the solution of a number of optimization problems [10,11]. In addition, their electronic implementation

[6,10,11] makes them attractive candidates for use in multilevel associative memories. Multilevel neurons' applications have also been reported in an optoelectronic implementation and applied to the smoothing of an image [12]. An experiment reported below shows the potential for GHNs for multilevel image noise removal.

A network shown in Fig. 4, with $N = 7$ was used for an image smoothing experiment. This network has eight stable states, namely $(-1, -1)$, $(-\frac{5}{7}, -\frac{5}{7})$, $(-\frac{3}{7}, -\frac{3}{7})$, $(-\frac{1}{7}, -\frac{1}{7})$, $(\frac{1}{7}, \frac{1}{7})$, $(\frac{3}{7}, \frac{3}{7})$, $(\frac{5}{7}, \frac{5}{7})$, and $(1, 1)$. The eight grey levels of a 250×200 image are mapped linearly onto the range $[-1, 1]$. Random noise values in the range $[-\frac{1}{7}, \frac{1}{7}]$ are now added to the mapped pixel values to produce a distorted image, giving the resulting image with noise superimposed in Fig. 13(a).

In order to verify the image smoothing performance of the network both v_1 and v_2 are initialized identical with the value of a distorted pixel and the network has been allowed to converge. The resulting (v_1, v_2) pair was then mapped onto a scalar value by taking their average. The images obtained for $\lambda = 3$, 5 and 50 are shown in Fig. 13(b), (c) and (d). Both $\lambda = 3$ and $\lambda = 5$ are subcritical since $\lambda_{Ecrit} = 12.4353$ for $N = 7$. These effects can be seen in the inaccurate smoothing of the image with very inaccurate smoothing for $\lambda = 3$, as expected. For $\lambda = 50 > \lambda_{Ecrit}$ it can be seen that the smoothing is perfect.

8. Conclusions

A qualitative analysis of the class of generalized Hopfield networks has demonstrated the existence of very useful dynamical neural network models. The proposed network requires a minimal number of weights and its processing power lies in the neuron's activation function. Due to the special nonlinearity of the network's characteristics, multiple local minima intertwined with saddles exist in the energy functions of a generalized bi-stable flip-flop configuration. Conditions for the existence of such minima and saddles have been developed. Dynamical properties have also been formulated in terms of the network energy function and discussed in terms of the gradient vector fields and basins of attraction. While the qualitative importance of these networks is in the sense that they generalize the bistable Hopfield networks, they are also of fundamental importance in many applications of dynamical neural systems as useful

(a) (b) (c) (d)

Fig. 13. (a) Noisy image and Resultant images from the image smoothing experiment (b) $\lambda = 3$ (c) $\lambda = 5$ (d) $\lambda = 50$.

computational devices. The applicability of the proposed network is demonstrated by means of a grey level image restoration example where each neuron assumes one of eight values. The proposed network behaves as a multistable memory cell and has tremendous potential as an information storage element in which a multiplicity of logic levels can be stored. Other applications may include multilevel associative memories and multivalued logic processors.

References

[1] J.J. Hopfield, Neurons with graded responses have collective computational properties like those of two state neurons, *Proc. Natl. Acad. Sci. USA* 81 (1984) 3088–3092.

[2] J.J. Hopfield and D.D. Tank, Computing with neural circuits: A model, *Science* 233 (1986) 625–633.

[3] J.M. Zurada, and M.J. Kang, Stationary points of single-layer feedback neural networks, *Proc. 1992 IEEE Int. Symp. on Circuits and Systems*, San Diego, CA (May 10–13, 1992) 57–60.

[4] W. Banzhaf, A network with multistable units capable of associative memory and pattern classification, *Physica D* 34 (1989) 418–426.

[5] J. Si and A.N. Michel, Analysis and synthesis of discrete-time neural networks with multilevel threshold functions, *Proc. 1991 IEEE Int. Symp. on Circ. and Syst.*, Singapore (June 1991), 1461–1464.

[6] J.D. Yuh and R.W. Newcomb, A multilevel neural network for A/D conversions, *IEEE Trans. Neural Networks* 4, (3) (May 1993) 470–483.

[7] J.M. Zurada, *Introduction to Artificial Neural Systems* (WPS, Boston, MA, 1992).

[8] D. Martland, Dynamic behavior of Boolean networks, in '*Neural Computing Architectures*', I. Alexander, ed. (MIT Press, Cambridge, MA 1989).

[9] J.M. Zurada, M.J. Kang and P.B. Aronhime, Vector field analysis of single layer feedback neural networks, *Proc. Midwest Symp. on Circuits and Systems*, Calgary, Canada (Aug. 12–14, 1990) 22–24.

[10] S.H. Bang, B.J. Sheu and J.C.-P. Chang, Multi-level neural networks with optimal solutions, to be published in *IEEE Trans. Circuits and Systems*, Part II.

[11] B.W. Lee and B.J. Sheu, Modified Hopfield neural networks for retrieving the optimal solutions, *IEEE Trans. Neural Networks* 2 (1) (Jan. 1991) 137–142.

[12] W. Zhang, K. Iloh, J. Taniba and Y. Ichioka, Hopfield model with multistate neurons and its optoelectronic implementation, *Applied Optics* 30 (2) (Jan. 1991) 195–200.

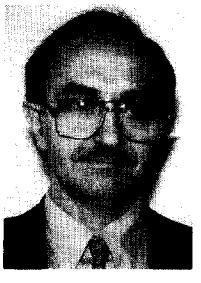

Jacek Zurada is the S.T. Fife Alumni Professor of Electrical Engineering at the University of Louisville, Louisville, Kentucky. He is the author of the 1992 PWS text *Introduction to Artificial Neural Systems*, contributor to the 1993 and 1994 Ablex volumes *Progress in Neural Networks*, and co-editor of the 1994 IEEE Press volume *Computational Intelligence: Imitating Life*. He is the author or co-author of more than 100 journal and conference papers in the area of neural networks, analog and digital VLSI circuits, and active filters. Dr. Zurada is now an Associate Editor of *IEEE Transactions on Neural Networks*, of *IEEE Transactions on Circuits and Systems, Part II, Neurocomputing*, and of the *Artificial Neural Networks Journal*. Dr. Zurada received a number of awards for distinction in research and teaching, including the 1993 Presidential Award for Research, Scholarship, and Creative Activity, and in 1994 he was the recipient of the Japanese Society for Promotion of Science Fellowship.

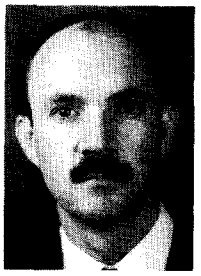

Ian Cloete is an Associate Professor of Computer Science at the University of Stellenbosch since 1993. He was previously employed at the National Accelerator Centre, responsible for the development of the computer control system. He obtained the M.Sc.Eng. degree from the University of Natal in 1983. After completing the Ph.D.Eng. degree at the Department of Electronic Engineering (University of Stellenbosch) in 1987, his academic career started in 1988 at the Department of Computer Science. He currently leads a research group on Neural Networks and Machine Learning. He is a senior member of the IEEE and a member of ACM Working Group 10.6 on Neural Computer Systems. Since 1992 he has received a Young Scientist research award from the South African Foundation for Research Development.

Etienne van der Poel received the B.Sc. degree in 1989 and the M.Sc. degree in Computer Science in 1992, both from the University of Stellenbosch, South Africa. He is currently pursuing a doctorate in Computer Science having received the prestigious SASOL (South African Synthetic Oil company) Research Sponsorship. His areas of research interest include Artificial Neural Networks and Scientific Visualization.